Electrochemistry Communications 11 (2009) 1449–1452

Contents lists available at ScienceDirect

Electrochemistry Communications

journal homepage: www.elsevier.com/locate/elecom

Enhanced stability and activity of PtRu nanotubes for methanol electrooxidation

S. Garbarino, A. Ponrouch, S. Pronovost, D. Guay *

INRS-Energie, Matériaux et Télécommunications, 1650 Boulevard Lionel Boulet, C.P. 1020, Varennes, QC, Canada J3X 1S2

ARTICLE INFO

Article history:
Received 18 April 2009
Received in revised form 14 May 2009
Accepted 14 May 2009
Available online 18 May 2009

Keywords:
Methanol
PtRu
Nanotube
Electrocatalysts
Electrooxidation

ABSTRACT

PtRu 1D nanostructures on titanium are prepared and analysed as electrocatalysts for methanol electrooxidation. The morphology and composition of the 1D nanostructure are characterized by scanning electron microscopy (SEM) and energy dispersive X-ray spectroscopy (EDS). The electrocatalytic properties of such catalysts for methanol oxidation are investigated by cyclic voltammetry (CV) and chronoamperometry (CA) in 1.0 M CH_3OH + 0.5 M H_2SO_4 aqueous solution. The results show that $Pt_{46}Ru_{54}$ nanotubes yields to a five-fold improvement of the mass specific activity and to a three-fold improvement of the long-term poisoning rate as compared to PtRu black of similar composition.

1. Introduction

Direct methanol fuel cell (DMFC) remains a promising portable source of energy, as the inexpensive fuel is stored in a liquid form, with a power density comparable to hydrogen/air polymer electrolyte membrane fuel cell near ambient conditions [1]. The most challenging improvements that need to be achieved for DMFC to reach the market are related to energy conversion efficiency, long-term stability and cost, and significant research activities have been targeted over the past years to reach that goal [2,3].

While it is considered that Pt is the best catalyst for the chemisorption of methanol, the poisoning of the platinum by methanol intermediates such as CO-type species impedes a high operating voltage. Enhanced methanol electrooxidation activity at bimetallic Pt–Ru catalysts has been extensively reported and was explained in terms of both the bifunctional mechanism and electronic effect [4]. Nevertheless, the optimum Ru content remains controversial, varying from 10 at.% [5–7] to 50 at.% [8–10].

It is hypothesized that the properties of 1D nanostructure make them less vulnerable than nanoparticles to dissolution and aggregation during fuel cell operation. Moreover, the anisotropic morphology of 1D nanotube was recently found to improve mass transport and catalyst utilization [11]. In this study, PtRu 1D nanowires and nanotubes within the above-mentioned composition range were prepared by potentiostatic electrodeposition through an AAO membrane. It is shown that PtRu nanotubes have a higher activity and are less prone to poisoning during methanol electrooxidation, as compared to PtRu black of similar composition.

2. Experimental

PtRu was electroplated on Ti substrates that were prepared as described previously [12]. Three different types of deposit were performed, namely PtRu black (B), nanowires (NW) and nanotubes (NT). In each case, the electroplating solution was [HCl] = 10 mM and $[Na_2PtCl_6{\cdot}xH_2O] = A$ mM + $[RuCl_3, 6H_2O] = B$ mM (Alpha Aesar) with A and B varying from 0.5 to 4.5 and $A + B = 5$. PtRu blacks were obtained by electrochemical deposition on bare Ti substrates, whereas NWs and NTs were prepared by deposition through a porous anodic aluminum oxide (AAO) membrane. All deposits were performed in potentiostatic mode at $E_d = -0.05$ V *vs* RHE and with a constant deposition charge density of 40 C cm^{-2}. Following deposition, the AAO membrane was dissolved by immersion in 1 M NaOH for 2 h at room temperature. All deposits were performed using a potentiostat–galvanostat Solartron SI 1287. The morphology of the deposits was observed using a scanning electron microscope (SEM, JSM-6300F, JEOL). The bulk atomic composition was determined by energy dispersive X-ray spectroscopy.

The electrochemical measurements were carried out at room temperature in a three-compartment glass cell. The auxiliary and the reference electrode were a Pt gauze and a reversible hydrogen electrode (RHE), respectively. All potentials are referred to that scale. Cyclic voltammograms (CVs) were recorded in de-aerated (Argon N5.0, Praxair) 0.5 M ultra pure sulphuric acid (A300-212, Fisher Scientific). Before each measurement, the electrode potential was cycled several times at 50 mV s^{-1} from 0.00 to 0.85 V.

---

* Corresponding author.
E-mail address: daniel.guay@emt.inrs.ca (D. Guay).

1388-2481/$ - see front matter Crown Copyright © 2009 Published by Elsevier B.V. All rights reserved.
doi:10.1016/j.elecom.2009.05.028

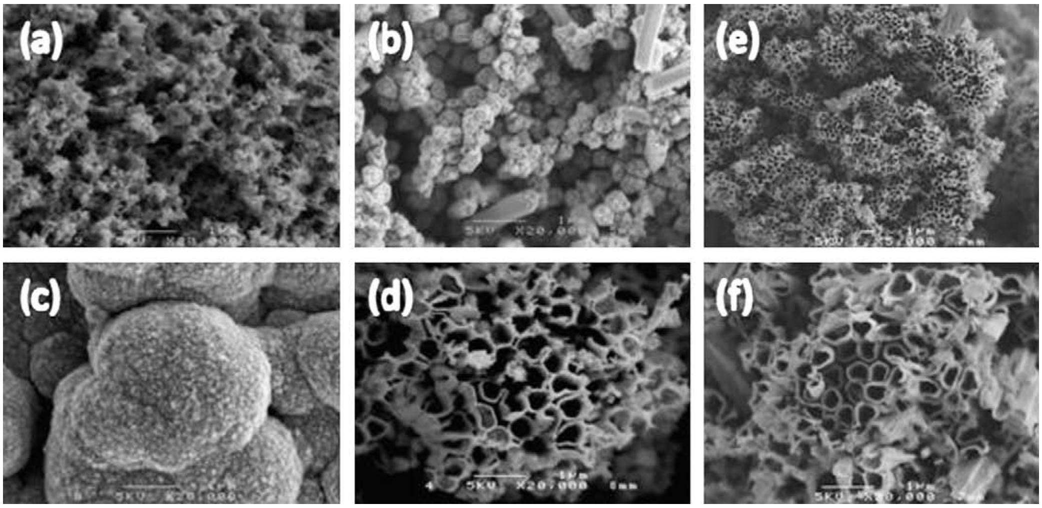

Fig. 1. Scanning electron microscopy micrographs of PtRu deposits prepared at −0.05 V. In (a) and (b), the Pt salt concentration was 2.5 mM, while it was 0.5 mM in (c) and (d). The electrodeposition was performed without (a and c) and with (b, d, e and f) an AAO membrane. The composition of the deposits are (a) $Pt_{87}Ru_{13}$, (b) $Pt_{85}Ru_{15}$, (c) $Pt_{41}Ru_{59}$, and (d, e and f) $Pt_{46}Ru_{54}$. The SEM micrographs of as-deposited electrodes are shown in (a, b, c and d), while those of electrodes after 1 h of electrolysis is methanol are shown (e and f).

The scan rate was then adjusted to 5 mV s^{-1} and the CV was recorded. The methanol (A412-4, Fisher Scientific) concentration was fixed at 1.0 M. The upper potential limit was set to 0.85 V as (i) no Pt surface restructuration and/or oxide growth occur to any significant extent below 0.9 V [13,14]; (ii) the onset of Ru dissolution from pure Ru [15] and from PtRu alloys [13] occurs at potentials above ca. 0.9 V; (iii) irreversible Ru oxides formation starts at potential higher than 0.9 V [16]. In the following sections, all results were normalized with respect to the mass of the deposit.

3. Results and discussion

SEM micrographs of typical PtRu deposits are presented in Fig. 1. The composition of the deposits varies with the concentration of the metal salts in the electroplating bath solution. In Fig. 1a and Fig. 1c, no AAO membrane was inserted at the Ti/electroplating solution interface and the micrographs are typical of PtRu black deposits with a porous structure at low Ru content and more uniform and globular structure at higher Ru content [6]. In contrast, long PtRu NWs (Fig. 1b) and NTs (Fig. 1d) are observed when deposition is performed through an AAO membrane. In our experimental conditions, PtRu NWs are obtained for [$Na_2PtCl_6{\cdot}xH_2O$] varying from 1.0 to 4.5 mM, while PtRu NTs are formed at [$Na_2PtCl_6{\cdot}xH_2O$] = 0.5 mM. In all cases, the X-ray diffraction patterns (not shown) indicate that a true PtRu solid solution is formed. The mechanisms responsible for the formation of metallic NWs and NTs are discussed elsewhere [17].

Cyclic voltammetric curves in sulphuric acid solution of $Pt_{41}Ru_{59}$ B and $Pt_{46}Ru_{54}$ NTs are displayed in the inset of Fig. 2a. These curves are similar to those presented in the literature [5,18] and they exhibit (i) a hydrogen sorption region from 0.00 to 0.35 V (Q^{H}_{PtRu}) and (b) a relatively featureless current region from 0.35 to 0.85 V. The current in that latter region is larger than observed on pure Pt and is attributed to the formation and reduction of oxide at ruthenium surface atoms (Q^{OH}_{Ru}). It is straightforward to conclude from these curves that the 1D structure directly influence the electrochemically accessible surface area, as both hydrogen sorption and double layer charging currents are superior for $Pt_{46}Ru_{54}$ NTs as compared to $Pt_{41}Ru_{59}$ B.

Cyclic voltammetric curves in sulphuric acid solution were analysed to identify a voltammetric feature, θ, sensitive to the presence of Ru at the surface of the catalyst. Following [9], θ is defined as:

$$\theta = Q^{OH}_{Ru}/Q^{H}_{PtRu} \qquad (1)$$

with Q^{OH}_{Ru} and Q^{H}_{PtRu} being the coulombic charges corresponding to the OH adsorption on ruthenium and to total surface hydrogen species desorption, respectively.

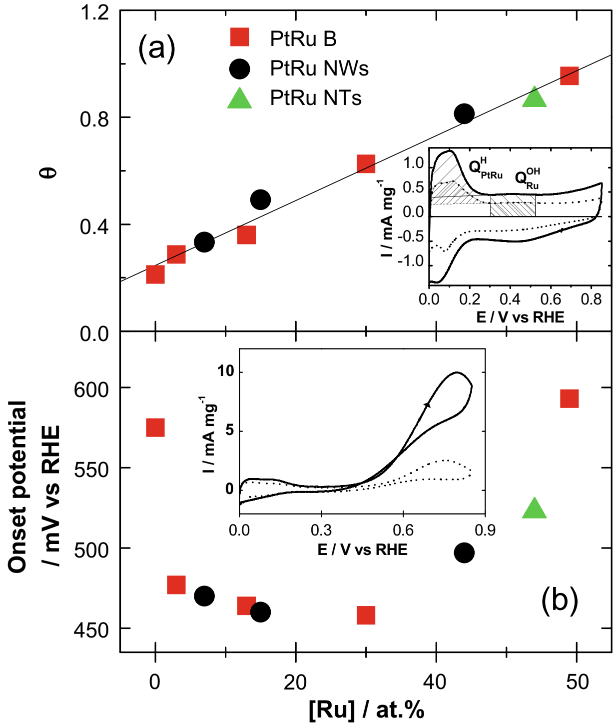

Fig. 2. Variation of (a) θ and (b) the onset potential for methanol electrooxidation with respect to the bulk Ru concentration. In (a), the insert displays the CVs of $Pt_{46}Ru_{54}$ NT (full line) and $Pt_{41}Ru_{59}$ B (dashed line) recorded in 0.5 M H_2SO_4 electrolyte at 5 mV s^{-1}. The dashed regions indicate how Q^{OH}_{PtRu} and Q^{H}_{Ru} were calculated. In (b), the insert displays the CVs of $Pt_{46}Ru_{54}$ NT (full line) and $Pt_{41}Ru_{59}$ B (dashed line) recorded in 0.5 M H_2SO_4 and 1 M CH_3OH at 5 mV s^{-1}.